

Wetland Soil Strength Tester and Core Sampler Using a Drone

Victor M. Baez¹, Shreyas Poyrekar¹, Marcos

Abstract—Soil strength testing and collecting soil c wetlands is currently a slow, manual process that risk of disturbing and contaminating soil samples. I describes a method using an instrumented dart dep retrieved by a drone for performing core sample te soils. The instrumented dart can simultaneously con fall penetrometer tests. A drone-mounted mechanis deploying and reeling in the dart for sample retu multiple soil strength tests. Tests examine the effect (diameter and drop height on soil retrieval, and the pull force to retrieve the samples. Further tests ex: dart's ability to measure soil strength and penetrati Hardware trials demonstrate that the drone can i drop and retrieve a dart, and that the soil can be sampled.

I. INTRODUCTION

Salt marshes are wetlands flooded periodically by tides and dominated by grasses. They occupy the land-sea boundary and survive rising seas by accreting soil. However, the ability of salt marshes to accrete soil is rate-limited, causing coastal erosion due to sea-level rise [1]. Knowledge gaps limit predictive understanding of the interactions between plants, the soil matrix, and the dynamic physical environment that drives the response of salt marshes to climate change.

Coastal soils are exposed daily to wet/dry cycles from tides. These dynamics present monumental challenges for generating adequate datasets in support of accurate modeling of large-scale ecosystem behavior. Even when exposed at low tide, it is often not possible to sample soils within a few meters from the marsh edge by boat or on foot without destroying the physical substrate and contaminating the chemistry. The collection of soil physical-chemical data remains limited primarily to destructive sampling of soil cores or pore water pressures caused by trekking through the soft substrate. Collecting soil cores on the coast is especially important because they provide valuable data on plant productivity, sediment accretionary dynamics, bulk densities, grain size distribution, and organic content [2]–[6]. *In situ* sensing approaches with the potential to rapidly evaluate wetland soil properties over large spatial scales represent an excellent opportunity to overcome these obstacles and improve predictive understanding of ecosystem-scale behavior.

*This work was supported by National Science Foundation (NSF) Grants No. [1646607, 1553063, 1849303] and the Hurricane Resilience Research Institute (HURRI).

¹ Authors are with the Department of Electrical and Computer Engineering, University of Houston, Houston, TX 77204 USA {atbecker, vjmontano, srpoyrekar, meibarramontoya, yahaikal}@uh.edu

² Author is with the Department of Civil and Environmental Engineering, Louisiana State University, Baton Rouge, LA 70803 USA njafari@lsu.edu

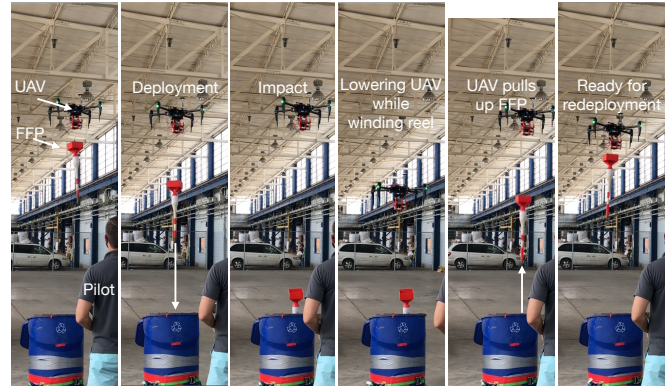


Fig. 1: Frames from video of a deployment sequence where the penetrometer was deployed and retrieved twice in succession. Full video at <https://youtu.be/8dLXEaZiFE>.

Moreover, a swarm of robots could enable multiple repeated *in situ* tests to rapidly evaluate soil properties, eliminating many drawbacks involved with access to ship time and the invasive nature of field core sampling, while decreasing the overall number of core samples required.

This paper focuses on the design, experimental study, deployment and retrieval system of our free fall penetrometer (FFP). Our FFP is a soil strength tester and a soil core sampler. This system is demonstrated in Fig. 1. Such a system could improve knowledge of coastal soils by enabling soil sampling and strength testing with greater precision and spatial scale. Using an Unmanned Aerial Vehicle (UAV) to deploy and retrieve the FFP would result in minimal environmental disturbance.

This paper extends the work of [7], which introduced a drone-delivered penetrometer dart with an integrated accelerometer, and examined the forces required to pull such a dart from the soil. In that paper, there was no mechanism to retrieve and redeploy the dart. There are three primary contributions of this study: (1) we provide a drone-based system for remotely performing repeated penetrometer tests. (2) We analyze using a FFP to collect soil cores. (3) We demonstrate and analyze a drone-based system for collecting multiple soil samples at discrete depths. This study also improves on the FFP design with higher-resolution accelerometer readings, and onboard sensing to measure penetration depth.

II. RELATED WORK

Soil geotechnical engineering properties are commonly quantified using a cone penetrometer. A cone penetrometer is a rod with a conical tip that is driven into the ground at a constant rate. Incorporated sensors log the required force to drive the rod [8]. A cone penetrometer is typically mounted on a heavy truck, but this setup is unsuitable for soft soils and underwater environments.



Fig. 2: The goal of soil cores is to collect an undisturbed soil sample. In the left image is a Shelby tube sampler, a metal tube that is pushed into the soil and pulled out to remove a soil core. Our hollow cylindrical dart tips are shown on the right. These cylinders are modular, and can be extended to match the soil properties (The first sections for two different diameter tips are :

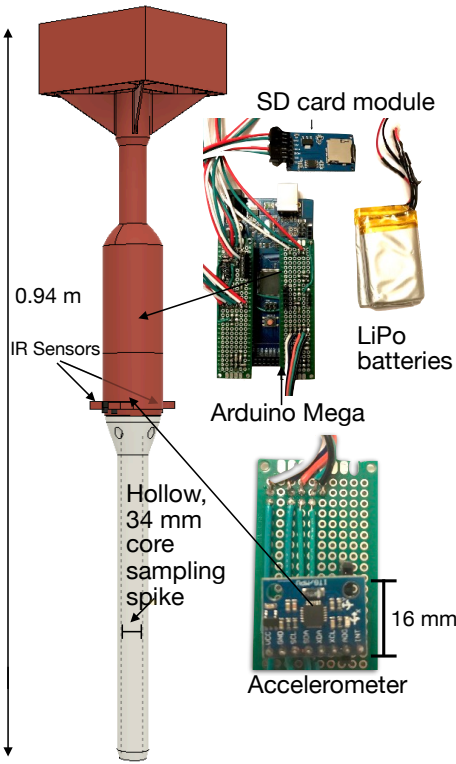


Fig. 3: Rendering of dart used for drop testing featuring the hollow 34 mm inner diameter core-sampling spike. Inside it contains an SD card module, a 16 g accelerometer, and two 3.7 V LiPo batteries connected to an Arduino Mega.

The sensing dart in this study derives some of its design from early free fall penetrometers (FFP), which were developed to measure the strength of seafloor sediments [9]. The seafloor FFP is a dart dropped into the ocean and allowed to accelerate to a terminal velocity (free fall). An onboard accelerometer measures the deceleration of the dart on impact. This data can be interpreted to measure the depth of penetration and the resistance of the soil.

Recent work involving UAV-deployed sensors include [10]–[13]. UAVs have been employed for collecting water samples [14]–[17], volcanic gas [18], and ice cores from

icebergs [19]. Work in [10] fired sensor darts into trees, but these sensors are left embedded in the tree and cannot be reused by the drone unless they are manually removed. UAVs have been used to drill out and retrieve ice cores from icebergs in [19]. In [14], samples of water were taken using a UAV to lower a weighted, water-collecting sleeve 122 m into a body of water. To collect soil core samples, however, penetrating the soil is necessary, as shown in Fig. 2. Penetration requires the sensor dart to move very rapidly, which is accomplished by dropping it from a height. A reel mechanism is necessary to enable repeated tests. This paper examines a dart-based soil sampling technique that can embed a dart into soil, perform measurements during impact, collect soil samples, and can also be retracted to repeat the process in different locations.

III. HARDWARE AND ENVIRONMENT

A. The free-falling penetrometer dart

Our new dart contains a 16 g accelerometer (MPU6050), an SD card module, two 3.7 V LiPo batteries, and a switch. It also has two IR sensors located diametrically opposite to each other on the outside of its shell. The electronics are connected to an Arduino Mega (Atmega2560), sampling the accelerometer at a rate of 400 Hz. The dart is 0.94 m long and has a total weight of 850 g. As in [7], the accelerometer is placed so one of its axes is aligned with the long axis of the dart, and the electronics were placed so their center of mass was aligned to the same axis.

This dart features interchangeable tips for comparisons in our experiments. Two of the tips, designed for outward core sampling, are hollow and have vents near the top for airflow during core sampling. The core-sampling tips are 450 mm long. This length is sufficient for dropping the FFP from a 3 m height without burying the air vents. The inside diameters of the two hollow tips are 22 mm and 34 mm and the shell walls are 3 mm thick. The last dart tip is a solid version of the larger diameter core sampling tip, having a diameter of 40 mm. An illustration showing the full dart featuring the 34 mm hollow core-sampling tip and electronics is shown in Fig. 3.

B. Retrieval mechanism

To drop one dart multiple times, we designed a retrieval mechanism based around a fishing reel. The reel (Abu Garcia Baitcast Silver Max 2) is sandwiched between two plates. A 0.2 kg-m servo (HiWonder LD-20mg) is used to press the release button, and a 12 V DC motor (131:1 Polulu Metal Gearmotor 37Dx73L) is used to wind the reel. The DC motor is attached to the handle of the reel through a gear train. This DC motor is driven by an L298N motor driver and powered using a 12 V LiPo battery. Both motors are controlled using a wireless transmitter/receiver (Frsky X9D). This design allowed for free fall of our dart, and repeated testing. The mechanism is shown in Fig. 4.

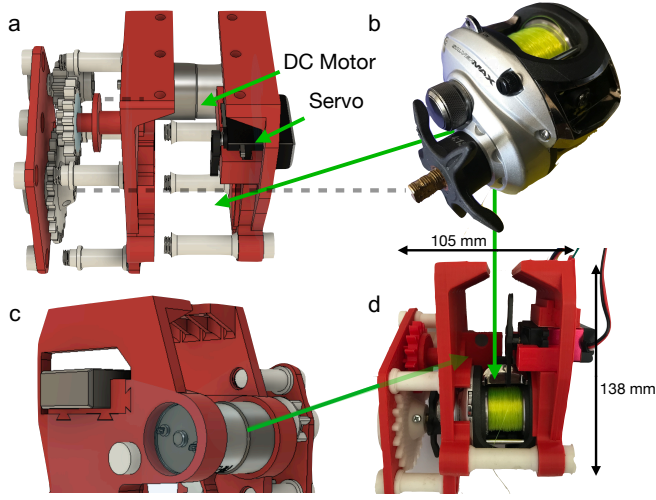


Fig. 5: Landscaping topsoil used for experiments. On the left is our dirt before mixing it with water to turn it into the mud on the right.

C. UAV

The drone tests used a Matrice 200 V2, which weighs 3.8 kg and has a rated flight time of 38 minutes. Our payload (0.75 kg for delivery and retrieval system + 0.85 kg for the instrumented dart) is within the rated payload of 2.0 kg. This UAV was used for the procedure in Subsection VI-A.

D. Tested soil

The soil we used in this study to simulate our wetland environment was produced by mixing water with fine-grained soils (silts and clays) until we reached a mud consistency, which serves as a proxy for a marsh soil. The gravimetric water content of the resulting soil was 20%. A picture of our soil before and after adding water is shown in Figure 5.

IV. METHODS

A. Drop tests for various spike types at various heights

For each of our drop test experiments, our instrumented dart was raised to a drop height and released into a 170 L recycling bin using a pulley suspended by a rope. The drop heights were measured from the tip of the dart to the surface of the soil in the recycling bin. The drop heights tested

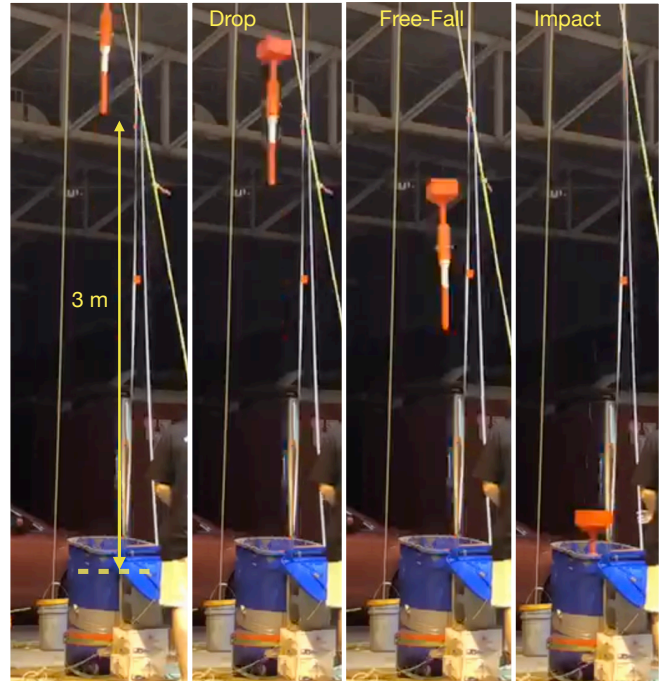


Fig. 6: Drop test from 3 m using the 34 mm inner diameter dart.

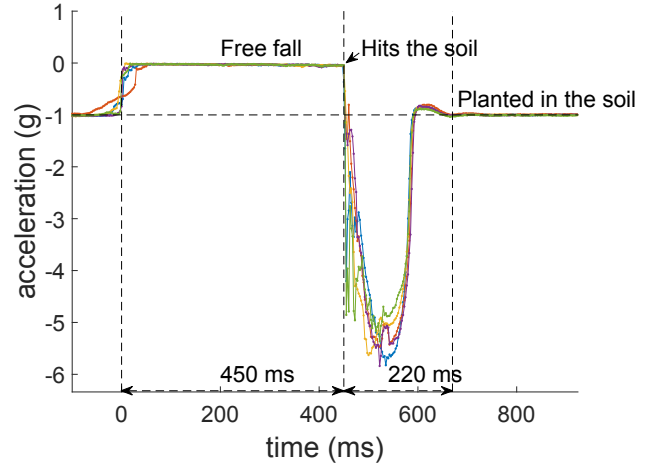


Fig. 7: Acceleration profile of five dart drops from a 1 m height (using the 22 mm inner diameter hollow spike). The free fall period (where the acceleration is 0g) is easy to detect, and this period T can be used to calculate the drop height ($\frac{1}{2}9.801T^2$). For the given $T = 0.451$ s, that height is 0.99 m.

were 1 m, 2 m, and 3 m. An example of a drop test from 3 m is shown in Fig. 6 and a representative timeline of the deceleration on impact is shown in Fig. 7. The displacement and velocity profiles are obtained by integrating and double integrating the deceleration, and is shown in Fig. 8.

B. Core sampling using a dropped dart

To collect core samples of our soil, we dropped our dart equipped with the 22 mm and 34 mm hollow inner diameter spikes. After each drop, we measured the penetration depth and the soil collection height in the core sampler. The dart was then carefully removed from the test soil, the spike was removed from the shell, and the collected soil sample was pushed and scraped through the opposite end using a rod into

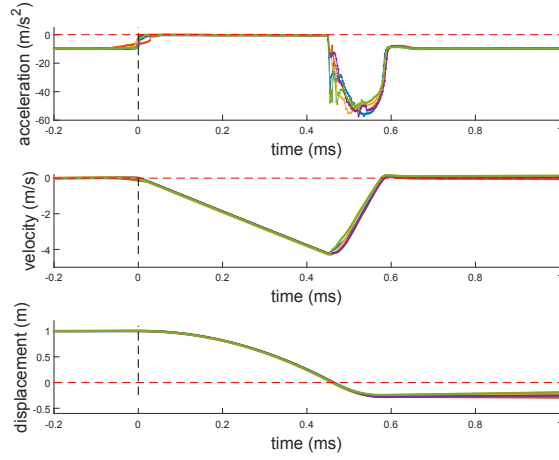


Fig. 8: Displacement, velocity, and acceleration profiles of five dart drops from 1 m height (using the 22 mm diameter hollow dart.)

a cup. Afterwards the soil sample was weighed on a scale.

C. Measuring pull forces required for a UAV

To measure pull forces required for a drone to remove a planted core sampler dart from our mud, we used a one-meter long linear actuator (OpenBuildsPartStore.com C-Beam) actuated by NEMA 23 stepper motor. The linear stage pulled on an S-type load cell (10 kg, CALT) fixed to the tail end of the dart at an average velocity of 72 mm/s. The stepper motor was controlled using an Arduino UNO (Atmega328p) and an L298N motor driver powered with 12 V and 2 A supply. The force was measured and logged by interfacing a load cell amplifier HX711 with a serial synchronous interface.

V. EXPERIMENTS AND RESULTS

Experiments in [7] show how the deceleration profile of a dropped dart is influenced by different soil types at various drop heights. Now that we are collecting core samples with dropped hollow spikes, we have compared the deceleration profiles between our core-sampling spike (34 mm inner diameter and 40 mm outer diameter) to a 40 mm solid spike to find out how this method of retrieving soil samples affects the impact deceleration. Tests were also performed to determine how core sampling using a dropped core sampler is affected by drop height and core diameter; we also determine how penetration depth correlates to the amount of soil sampled.

A. Deceleration profiles of a hollow vs solid spike

To compare the deceleration profiles between a hollow core-sampling spike to a solid spike, both spike types were dropped from three different heights. Before each drop test, the wet soil was mixed, and the soil surface was flattened. After each drop test using the hollow spike, the core of mud was removed and the spike was cleaned. Drop tests were performed five times for both spike types. Figure 9 shows the resulting deceleration profiles. All show that the solid spike (shown in blue) experiences greater peaks in deceleration when dropped from 1 m and 3 m, and that

complete deceleration takes longer when using the hollow core-sampling spike (shown in red).

The experiment highlighted the significant difference in deceleration profiles between hollow spikes and solid spikes as used in [7]. This difference must be accounted for when using a core-sampling version of the FFP to measure soil resistances. Further analysis will be required to quantify these differences to adjust soil resistance measurements. The deceleration profiles grouped by dart type are shown in Fig. 10a and Fig. 10b.

B. Effects of core diameter on mud retrieval and penetration depth

Figures 11a and 13a show that even though a smaller diameter core sampler penetrates deeper into the soil, the larger diameter core sampler collects more soil. However, Subsection C describes why a smaller-diameter core sampler is more effective in soils having greater moisture content. Figure 11b shows that a hollow spike will penetrate deeper than a solid spike when dropped from the same height.

The penetration depth measured for five dart drops for a 22 mm inner diameter hollow dart is around 200 mm, as seen in Fig. 11a. This is approximately the displacement obtained by double integrating the deceleration profile as seen in Fig. 8. The deceleration profiles comparing different diameter hollow tubes are shown in Fig. 12a and 12b.

C. The maximum water content suitable for our core sampling retrieval

To determine the range of water content our core sampling method of retrieving soil works with, we started with 2 kg of the mud used in our drop experiments. We dipped the hollow spikes in the mud 0.5 m deep, pulled them out, and held them vertically for 30 seconds. We then mixed in 20 mg of water and repeated the procedure until mud slipped out of the hollow spikes. Mud started to slip out of the 34 mm inner diameter spike at 42% water content, while mud stayed inside the 22 mm inner diameter spike until a water content of 50%. In Section VI-B we demonstrate a sampling technique that also works with water content greater than 50%.

D. Force required to pull a hollow dart out of wet soil

A plot of the pull force required to pull out an FFP equipped with a 22 mm hollow spike tip is shown in Fig. 14. Using a 22 mm inner diameter hollow tip, the force required for retrieval spikes up to 13 kg. Though this force exceeds the rated maximum dynamic payload of the drone, it is for a short time period. After the dart is pulled from the mud, the load settles to nearly 2 kg, greater than the weight of the dart due to additional collected soil sample and wet soil stuck to the outside of the spike.

Alternate techniques to reduce the required pull force on the drone include pulling at different rates, pulling at an angle, and using a sacrificial sleeve, all discussed in [7].

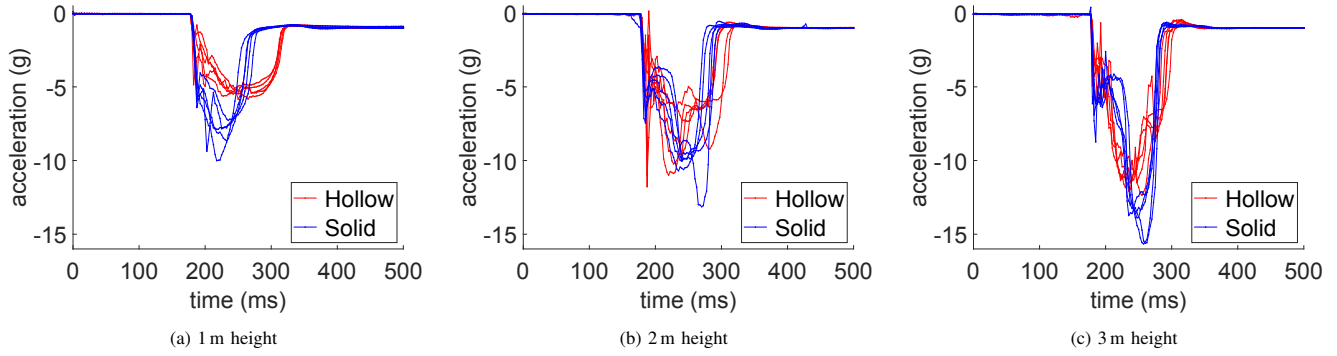


Fig. 9: Impact deceleration plots of the 40 mm outer diameter tips (solid, and 34 mm inner diameter hollow) from three different drop heights into soil.

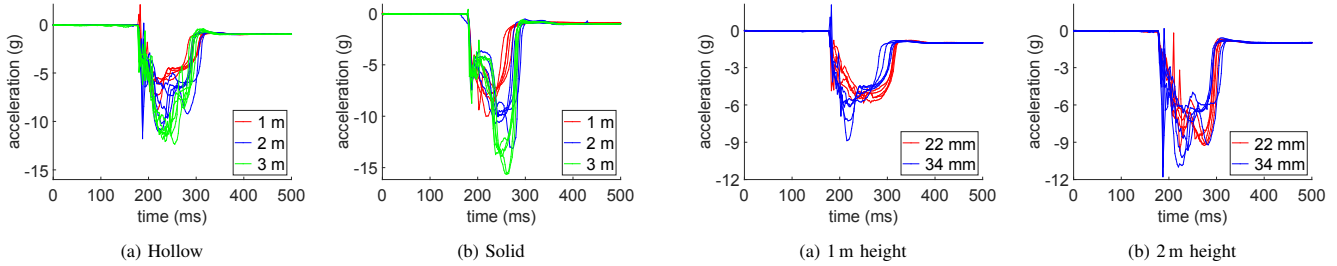


Fig. 10: Plot of the impact deceleration of the 34 mm inner diameter dart into soil for dart types with different drop heights.

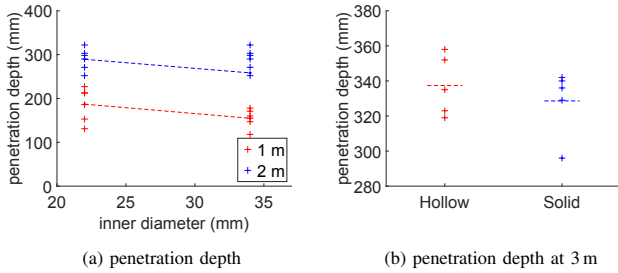


Fig. 11: (a) shows the penetration depth of the dart for two inner diameters dropped at two heights. (b) compares the penetration depths of a hollow and solid spike dropped from 3 m (both have a 40 mm outer diameter.)

VI. DEMONSTRATIONS

A. Successful deployment and retrieval

To reduce the payload on our UAV, a smaller and lighter version of the dart was used. The video attachment shows two successive deployments followed by two retrievals during one flight, demonstrating that the process is repeatable, and within the capabilities of a commercial, off-the-shelf drone. For these tests, a pilot with a remote pilot certificate flew the drone with the aid of two spotters. Six frames from this video are shown in Fig. 1, showing the flight, deployment, impact, reel winding, and UAV pulling steps.

B. Solution for taking samples of soil at multiple locations

The core-sampling dart tip presented in Sec. IV-B can only sample at one location. This section presents an alternate dart tip design that enables our FFP to take depth-registered soil samples at multiple locations using the same tip. Though each of these samples are only 0.8 mL, this amount of soil is suitable for supporting microbiological and geochemical characterization. The procedure is illustrated in Fig. 15.

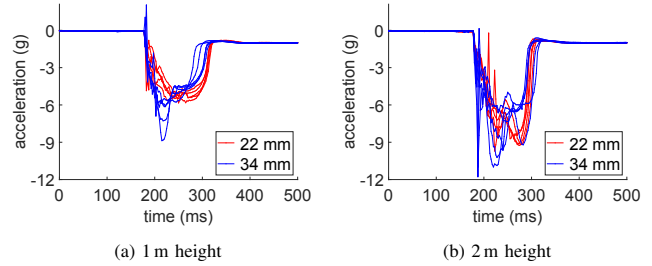


Fig. 12: Plot of the impact deceleration of the hollow dart tip from two drop heights into soil with different dart diameters.

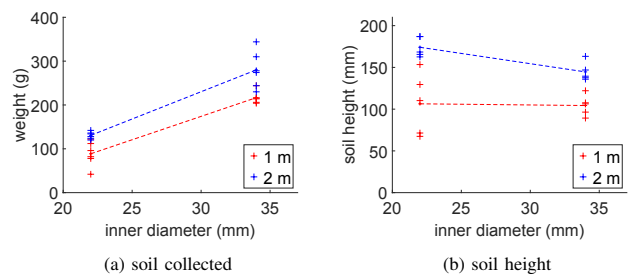


Fig. 13: (a) shows the weight of soil collected for two dart inner diameters dropped at two heights with hollow darts. (b) shows the height of the soil collected inside the sampler for two diameters at two drop heights with hollow darts.

The dart consists of an outer sheath and an inner rotating sampler. The sampler is actuated by an internal servo motor (Fig. 15a). The sheath has a single vertical column of eight sampling holes. These holes are beveled to slice through the soil in a design inspired by a medical biopsy robot [20]. The inner rotating sampler has four columns of sampling pockets that match the outer holes. Each pocket can hold 0.8 mL of soil. By rotating the inner sampler, different columns can be exposed to the outer soil. The dart is dropped with the pockets sealed. In our demonstration, we manually drove the dart tip into a jar of wet soil (Fig. 15 c). Once in the soil, the inner sheath is rotated to expose a column of pockets to the soil. After the sampler is in the soil, lateral earth pressure pushes samples into the pockets. After a predetermined wait time, the inner sampler rotates to seal off the pockets and the dart is ready for retrieval. In the future, this wait time could be defined by the soil type, where the soil type is determined by the deceleration profile.

For our demonstration illustrated in Fig. 15, a 0.2 kg-

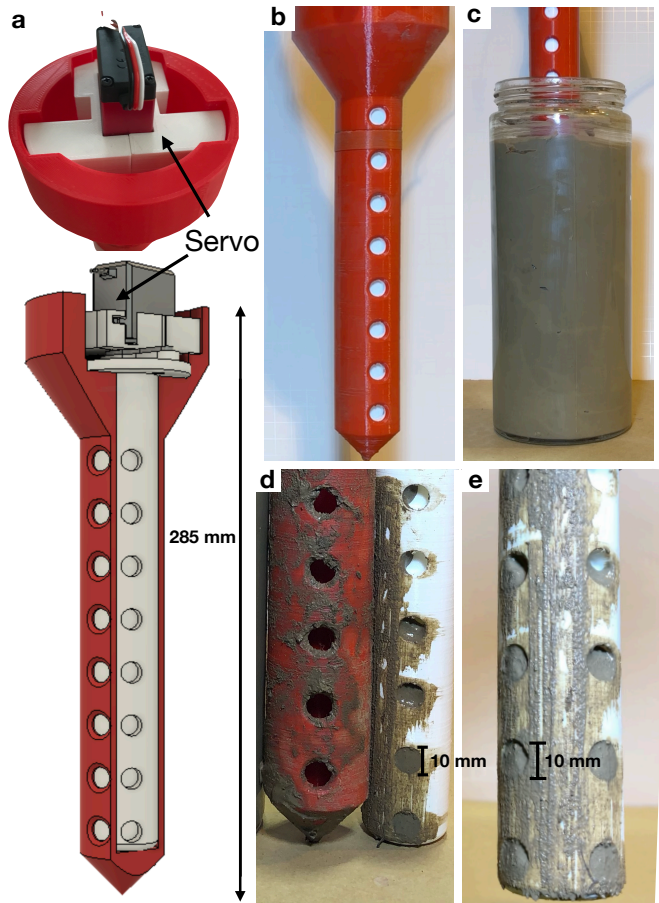
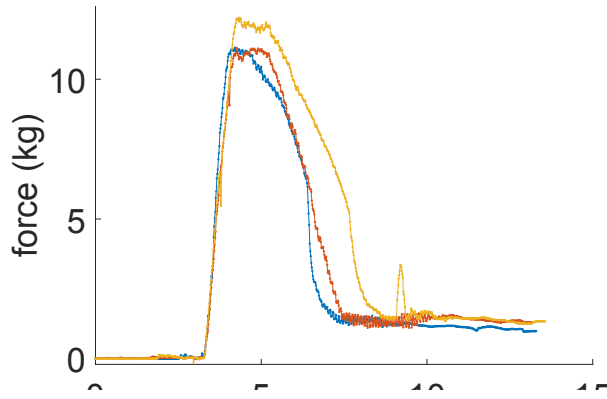


Fig. 15: Soil collection system: a) Rendering of actuated dart tip showing rotating sampler inside and actuating servo. b) Photo of dart tip before placing in jar of mud. c) After placing the dart tip in the mud, the servo was actuated to collect a sample. d) Disassembled dart tip showing the outer sheath and the inner rotating sampler with mud samples collected. e) Inner rotating sampler showing two columns of sampling pockets with collected mud inside. See video at <https://youtu.be/8dLXEaZiFE>.

m servo motor (HiWonder LD-20mg) was connected to a wireless receiver (X8R) and controlled with a wireless transmitter (FrskyX9D).

VII. CONCLUSION

This study addressed limitations in previous efforts (including [7]) by providing a remote method to perform multiple soil measurements and soil sampling using a UAV. The study specifically introduced a delivery and retrieval mechanism to drop an instrumented dart into soft soil and measure the deceleration profile and the penetration depth. The study demonstrated that the system enables a UAV to make multiple measurements. The dart is versatile and reconfigurable. The same dart design can be configured for collecting soil core samples, or for simultaneously collecting multiple soil samples at different penetration depths, and storing these in the dart for examination later.

Though this study established the feasibility of such a system, future efforts should focus on making the system robust and to study the best practices for conducting soil measurements with a team of UAVs over a large geographic area. Future prototypes could have added capabilities to measure surface elevation, soil salinity, heat or temperature, redox-active chemical species (O_2 , sulfide, Mn^{2+} , Fe^{2+}), and microbial dynamics. Improved sensing capability will facilitate a deeper understanding and modeling of the rate of soil accretion, the accumulation of soil organic matter, and plant productivity that determine the responses of salt marsh ecosystems to rising sea level.

ACKNOWLEDGEMENTS

Evan Headroe, Gerrit Nelson, and Mitch Presson aided in testing the reel prototype and the instrumented dart. We are grateful for the testing space provided by Saurabh Sogi and to Craig Glennie, Darren L. Hauser and Abhinav Singhania for piloting the drone.

REFERENCES

- [1] C. Wigand, C. T. Roman, E. Davey, M. Stolt, R. Johnson, A. Hanson, E. B. Watson, S. B. Moran, D. R. Cahoon, J. C. Lynch *et al.*, "Below the disappearing marshes of an urban estuary: historic nitrogen trends and soil structure," *Ecological Applications*, vol. 24, no. 4, pp. 633–649, 2014.
- [2] P. L. Wiberg, S. Fagherazzi, and M. L. Kirwan, "Improving predictions of salt marsh evolution through better integration of data and models," *Annual review of marine science*, vol. 12, pp. 389–413, 2020.
- [3] S. Fagherazzi, G. Mariotti, N. Leonardi, A. Canestrelli, W. Nardin, and W. S. Kearney, "Salt marsh dynamics in a period of accelerated sea level rise," *Journal of Geophysical Research: Earth Surface*, vol. 125, no. 8, p. e2019JF005200, 2020.
- [4] G. Mariotti, T. Elsey-Quirk, G. Bruno, and K. Valentine, "Mud-associated organic matter and its direct and indirect role in marsh organic matter accumulation and vertical accretion," *Limnology and Oceanography*, 2020.
- [5] R. R. Lane, S. K. Mack, J. W. Day, R. D. DeLaune, M. J. Madison, and P. R. Precht, "Fate of soil organic carbon during wetland loss," *Wetlands*, vol. 36, no. 6, pp. 1167–1181, 2016.
- [6] J. T. Morris, D. C. Barber, J. C. Callaway, R. Chambers, S. C. Hagen, C. S. Hopkinson, B. J. Johnson, P. Megonigal, S. C. Neubauer, T. Troxler *et al.*, "Contributions of organic and inorganic matter to sediment volume and accretion in tidal wetlands at steady state," *Earth's future*, vol. 4, no. 4, pp. 110–121, 2016.
- [7] V. M. Baez, A. Shah, S. Akinwande, N. H. Jafari, and A. T. Becker, "Assessment of soil strength using a robotically deployed and retrieved penetrometer," in *2020 IEEE/RSJ International Conference on Intelligent Robots and Systems (IROS)*. IEEE, 2020, p. tbd.
- [8] P. Robertson and K. Cabal, *Guide to Cone Penetration Testing For Geotechnical Engineering*, 6th ed. Signal Hill, California: Gregg Drilling & Testing, Inc., 2015.

- [9] M. Mumtaz, N. Stark, and S. Brizzolara, "Pore pressure measurements using a portable free fall penetrometer," in *Cone Penetration Testing 2018: Proceedings of the 4th International Symposium on Cone Penetration Testing (CPT'18), 21-22 June, 2018, Delft, The Netherlands*. CRC Press, 2018, p. 461.
- [10] A. Farinha, R. Zufferey, P. Zheng, S. F. Armanini, and M. Kovac, "Unmanned aerial sensor placement for cluttered environments," *IEEE Robotics and Automation Letters*, vol. 5, no. 4, pp. 6623–6630, 2020.
- [11] S. K. Sudarshan, L. Huang, C. Li, R. Stewart, and A. T. Becker, "Seismic surveying with drone-mounted geophones," in *2016 IEEE International Conference on Automation Science and Engineering (CASE)*. IEEE, 2016, pp. 1354–1359.
- [12] R. Stewart, L. Chang, S. Sudarshan, A. Becker, and L. Huang, "An unmanned aerial vehicle with vibration sensing ability (seismic drone)," in *SEG Technical Program Expanded Abstracts 2016*. Society of Exploration Geophysicists, 2016, pp. 225–229.
- [13] S. K. Sudarshan, V. Montano, A. Nguyen, M. McClimans, L. Chang, R. R. Stewart, and A. T. Becker, "A heterogeneous robotics team for large-scale seismic sensing," *IEEE Robotics and Automation Letters*, vol. 2, no. 3, pp. 1328–1335, 2017.
- [14] D. Castendyk, J. Voorhis, and B. Kucera, "A validated method for pit lake water sampling using aerial drones and sampling devices," *Mine Water and the Environment*, pp. 1–15, 2020.
- [15] J.-P. Ore, S. Elbaum, A. Burgin, and C. Detweiler, "Autonomous aerial water sampling," *Journal of Field Robotics*, vol. 32, no. 8, pp. 1095–1113, 2015.
- [16] M. Schwarzbach, M. Laiacker, M. Mulero-Pázmány, and K. Kondak, "Remote water sampling using flying robots," in *2014 International Conference on Unmanned Aircraft Systems (ICUAS)*. IEEE, 2014, pp. 72–76.
- [17] A. Terada, Y. Morita, T. Hashimoto, T. Mori, T. Ohba, M. Yaguchi, and W. Kanda, "Water sampling using a drone at yugama crater lake, kusatsu-shirane volcano, japan," *Earth, Planets and Space*, vol. 70, no. 1, pp. 1–9, 2018.
- [18] F. D'Arcy, J. Stix, J. de Moor, J. Rüdiger, J. Diaz, A. Alan, and E. Corrales, "Drones swoop in to measure gas belched from volcanoes," *EOS*, 2018. [Online]. Available: <https://eos.org/science-updates/drones-swoop-in-to-measure-gas-belched-from-volcanoes>
- [19] D. F. Carlson, J. Pasma, M. E. Jacobsen, M. H. Hansen, S. Thomsen, J. P. Lillethorup, F. S. Tirsgaard, A. Flytkjær, C. Melvad, K. Laufer, L. C. Lund-Hansen, L. Meire, and S. Rysgaard, "Retrieval of ice samples using the ice drone," *Frontiers in Earth Science*, vol. 7, p. 287, 2019. [Online]. Available: <https://www.frontiersin.org/article/10.3389/feart.2019.00287>
- [20] M. C. Hoang, V. H. Le, J. Kim, E. Choi, B. Kang, J.-O. Park, and C.-S. Kim, "Untethered robotic motion and rotating blade mechanism for actively locomotive biopsy capsule endoscope," *IEEE Access*, vol. 7, pp. 93 364–93 374, 2019.